Solid State Sciences 90 (2019) 14–20

Contents lists available at ScienceDirect

Solid State Sciences

journal homepage: www.elsevier.com/locate/ssscie

Structural evolution and electronic properties of CaS: An ab initio study

Cihan Kürkçü[a,*], Çağatay Yamçıçıer[b], Mustafa Kurban[a,**]

[a] Department of Electronics and Automation, Kırşehir Ahi Evran University, 40100, Kırşehir, Turkey
[b] Institute of Science, Gazi University, 06500, Ankara, Turkey

ARTICLE INFO

Keywords:
Phase transition
Enthalpy
Intermediate state
Electronic structure
Ab-initio

ABSTRACT

CaS crystallizes in cubic NaCl (B1) type structure with symmetry $Fm\bar{3}m$. In this work, the structural and electronic properties of CaS were investigated by considering the Density Functional calculations within the framework of Generalized Gradient Approximation (GGA) under high pressure. The structural change was found at the B1 type structure of CaS. B1 type structure transformed into another cubic CsCl (B2) type structure with symmetry $Pm\bar{3}m$ at 36.6 GPa. An intermediate state with symmetry $R\bar{3}m$ was predicted during this transition. Besides, the effects of the pressure on the electronic properties of CaS were also studied. Both the B1 and B2 type structures exhibited semiconducting behaviors with direct band gaps at the Γ-point and R-point, respectively. Intermediate state was searched during this phase change first time in detail. The obtained results were compared with experimental and theoretical ones in the literature.

1. Introduction

II–VI semiconductor compounds have recently attracted increasing interest in many applications, due to their effective use in light emitting diodes and infrared sensitive devices [1,2]. These compounds are commonly used in many electronic and optoelectronic devices such as solar cells, photodetectors, visual displays and high solid-state laser devices etc. Considering II–VI semiconductors, especially, calcium sulfide (CaS) is the most important representative due to its interesting properties such as high sensitivity to infrared radiations and high accumulation capability [3]. CaS has a wide bandgap semiconductor which is particularly important as a host material in many lighting applications [4–7].

Recently, the structural phase transformations have attracted considerable interest as it provides insight into the electronic structure and physical properties of solid state. At ambient pressure, CaS crystallizes in the rock-salt (B1) structure with space group $Fm\bar{3}m$. CaS crystal in the NaCl-type (B1) structure under pressure transforms into CsCl-type (B2) structure with space group $Pm\bar{3}m$. In addition, the crystal structure of CaS exhibits a structural first order phase transition under pressure of 40 GPa [8]. In the work, the metallization was also observed when the crystal structure of CaS compound undergoes a structural phase transition to the CsCl-type (B2) as based on the application of further pressure.

A fundamental understanding of physical and electronic properties of CaS compound is still in demand at pressure. Therefore, the main aim of this study is to search some physical properties and electronic structure such as the energy-volume curves, the volume change of the simulation cell, intermediate states during the phase change, total energy, enthalpy, band structure and density of states (DOS) and compare the obtained results with experimental and theoretical ones in the literature.

2. Methods

The Density Functional Theory (DFT) calculations were performed using the norm-conserving pseudopotential (Troullier-Martins) [9] implemented in the SIESTA program package [10]. The exchange and correlation energy were described with the Perdew-Burke-Ernzerhof (PBE) [11] form of the GGA. We used a $8 \times 8 \times 8$ Monkhorst-Pack [12] grid for k-point sampling in the Brillouin Zone (BZ) for zinc-blende, B1 and B2 structures of CaS. The geometric structure was obtained by relaxing all the atoms with residual force smaller than 0.01 eV/Å on each atom. The mesh cutoff energy was chosen to be 350 Ry, which means that all plane waves with a smaller kinetic energy than 350 Ry will be included in the basis set but those with a higher kinetic energy will be omitted in the basis set. Higher cut-off energies will give better results but the calculations will be more time consuming. A double-ζ basis including polarization orbitals were used. Pressure is gradually increased by 10 GPa by applying Parrinello-Rahman method to the

* Corresponding author.
** Corresponding author.
E-mail addresses: ckurkcu@ahievran.edu.tr (C. Kürkçü), mkurbanphys@gmail.com (M. Kurban).

https://doi.org/10.1016/j.solidstatesciences.2019.02.003
Received 1 January 2019; Received in revised form 15 January 2019; Accepted 5 February 2019
Available online 06 February 2019
1293-2558/

system. The KPLOT [13] program and the RGS [14] algorithm are used to analyze each molecular dynamic (MD) time step. They give detailed information about the space group, atomic positions and lattice parameters of an analyzed structure.

3. Results and discussions

CaS crystallizes in the cubic structure (B1) with the space group $Fm\bar{3}m$ under ambient conditions. This structure's lattice parameters were obtained to be $a = b = c = 5.7386$ Å at 0 GPa. The CaS has 8 atoms in the unit cell for B1 type structure. Ca atoms are located at positions 4*a* (0, 0, 0) and S atoms at 4*b* (1/2, 1/2, 1/2) positions. The B1-type structure of the CaS compound was first brought to equilibrium at a pressure of 0 GPa. Later pressure was applied up to 200 GPa by applying increments of 10 GPa on the B1-type structure of CaS. When the pressure was increased from 160 GPa to 170 GPa, it was observed that B1-type structure of CaS transformed into another cubic (B2-type) structure with space group $Pm\bar{3}m$. The lattice parameters of this B2-type structure at 170 GPa are $a = b = c = 3.4680$ Å. Ca atoms are located at positions 1*a* (0, 0, 0) and S atoms at 1b (1/2, 1/2, 1/2) positions We also calculated the zinc-blende structure with space group $F\bar{4}3m$ of CaS to compare with other B1 and B2 structures. This zinc-blende structure's lattice parameters were obtained to be $a = b = c = 6.5093$ Å at 0 GPa. The CaS has 8 atoms in the unit cell for zinc-blende type structure. Ca atoms are located at positions 4*a* (0, 0, 0) and S atoms at 4*c* (1/4, 1/4, 1/4) positions. The obtained zinc-blende, B1 and B2-type structures of CaS are given in Fig. 1 and the transition pressures, lattice parameters, bulk modulus and derivate of bulk modulus of B1 and B2-type structures are given in Table 1.

In order to determine the thermodynamic nature of the phase transformations for the CaS compound, the relations of pressure-volume, pressure-lattice constants and pressure-angles between *a*, *b* and *c* lattice parameters obtained during constant pressure ab initio simulations are shown in Fig. 2 a, b and c, respectively. As can be seen from Fig. 2 a, while the pressure value is increased from 160 GPa to 170 GPa for CaS, a sharp decrease in volume is observed. This shows us that there is a phase transition containing first order pressure.

Because the work we have done is carried out under hydrostatic pressure, the pressure value measured for transition from one phase to another phase is generally higher than the transition pressure values obtained from other experimental and theoretical calculations due to the important energy barrier that the material encountered during this transition. Therefore, simulated systems will want to overcome this energy barrier in order to transform to another structure having different symmetry. Thus, it will be exposed to a lot of pressure [15–18]. Therefore, in the next step, we took into account the energy-volume calculations to study the stability of the high pressure phases of CaS in Fig. 3. As seen from Fig. 3, the most stable structure of CaS is zinc-blende due to the it has the lowest energy. Calculated total energy-volume relations is fitted to the third-order Birch-Murnaghan equation of state [19,20] that given by

$$P = 1.5B_0\left[\left(\frac{V}{V_0}\right)^{-\frac{7}{3}} - \left(\frac{V}{V_0}\right)^{-\frac{5}{3}}\right]x\left\{1 + 0.75(B_0' - 4)\left[\left(\frac{V}{V_0}\right)^{-\frac{2}{3}} - 1\right]\right\} \quad (1)$$

where P is the pressure, V is the volume at the pressure, V_0, B_0 and B_0' are the volume, bulk modulus and its pressure derivate at 0 GPa, respectively.

At the given temperature and pressure value, Gibbs free energy (G) is used to determine which of the phases obtained from the study was most thermodynamically stable and is given as follows.

$$G = E_{tot} + PV - TS \quad (2)$$

where E is the total energy, P is the pressure, V is the volume and S is the entropy. This simulation study was achieved at a temperature of 0 K. Therefore, the term "TS" was neglected. Thus, Gibbs free energy G equals to the enthalpy as follows:

$$H = E_{tot} + PV \quad (3)$$

where $P = dE_{tot}/dV$.

Enthalpy calculations generally give the transition pressure values

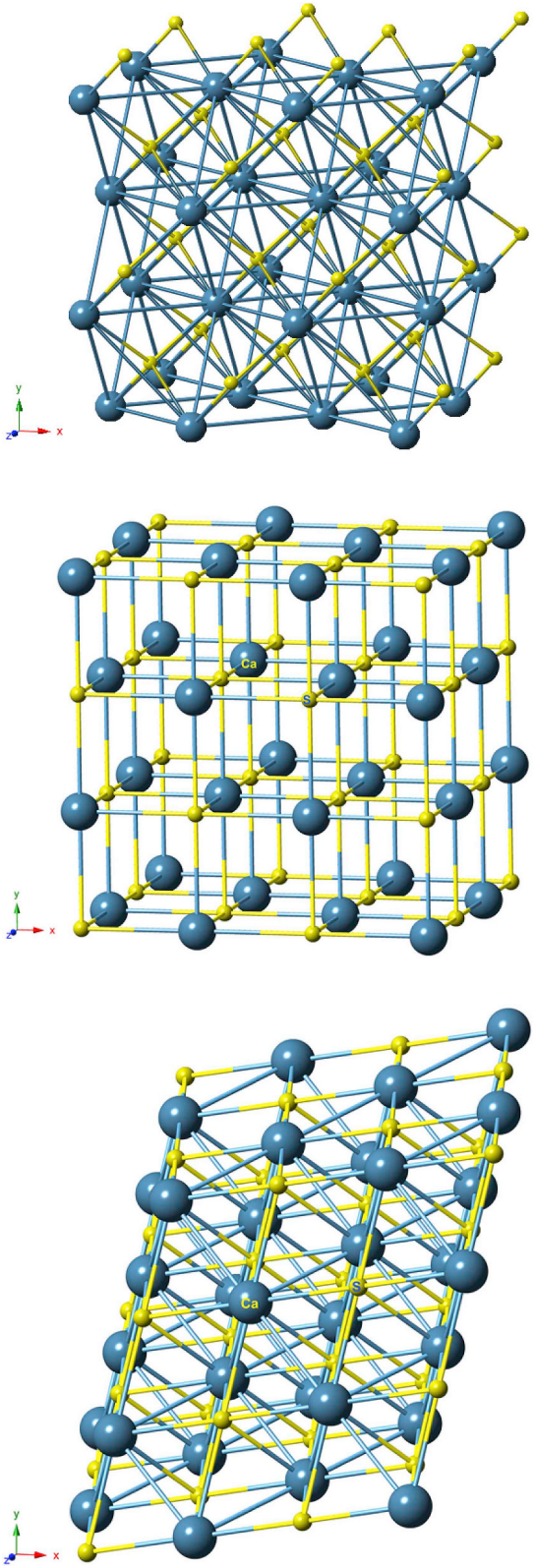

Fig. 1. Crystal structures of CaS: Zinc-blende structure (top) at zero pressure, B1 structure (middle) at zero pressure and B2 structure (bottom) at 170 GPa.

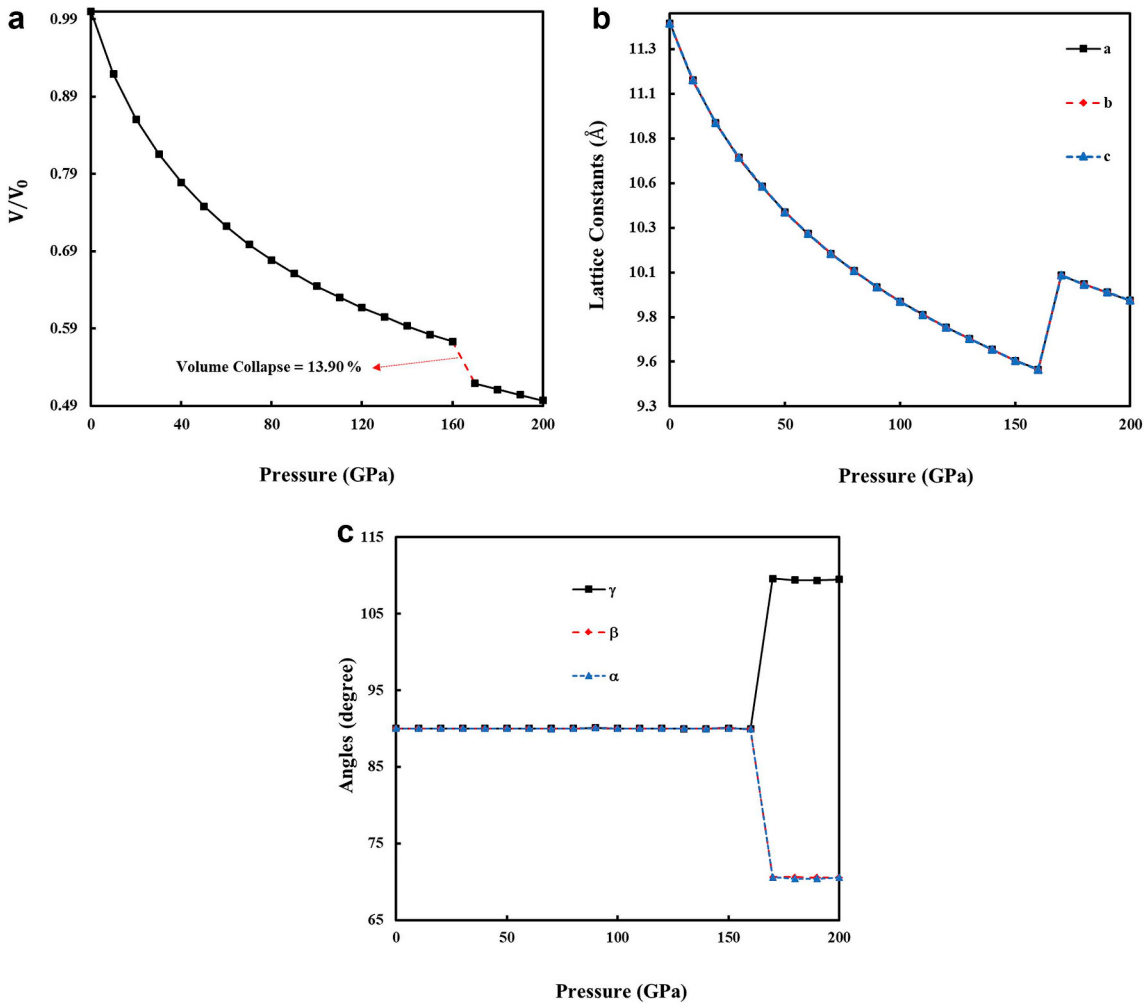

Fig. 2. The graph of the change of simulation cell volume (a), lattice constant (b) and angles (c) as function of the pressure.

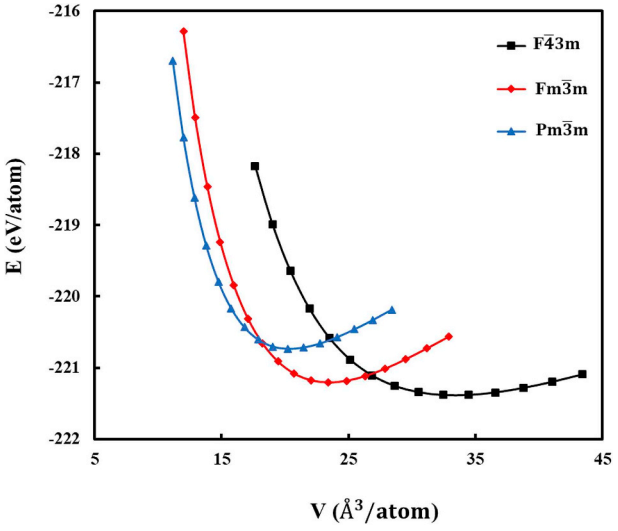

Fig. 3. Energy-volume graph of the stable structural phases of the CaS compound.

in good agreement with the experimental results. The intersection of the two enthalpy curves indicates the phase transition containing the pressure between these two phases. In order to determine the transition pressure, we plotted the enthalpy curve for the obtaining phases of CaS as the function of pressure, as shown in Fig. 4. We used energy-volume data to plot the enthalpy curve. As can be seen from Fig. 4, the transition pressure between the cubic B1 structure with the space group.

$Fm\bar{3}m$ and the another cubic B2 structure with the symmetry of $Pm\bar{3}m$ was obtained as 36.6 GPa. As shown in Table 1, the value of the transition pressure obtained from the enthalpy calculation is in agreement with other experimental and theoretical studies.

Later, to explain the mechanism of phase transitions, the lengths of the lattice vectors of the simulation cell and how the angles between these vectors change according to the simulation steps were examined. These vectors were denoted **A**, **B** and **C** along the directions [100], [010] and [001], respectively. The angles between **A** with **B**, **A** with **C** and **B** with **C** were expressed as gama, beta and alfa, respectively. The variation of lattice vector lengths and the angles between these vectors was shown for 170 GPa in Fig. 5 (a) and (b).

From Fig. 5 (a) and (b), the α, β, γangles remain constant up to about 100^{th} MD time step. Then the γ angle starts to increase at around 150^{th} MD time step and after reaching about 110^0, they remain unchanged through the simulation. The α and β angles start to decrease at around 150^{th} MD time step and after reaching 70^0, they remain unchanged through the simulation. The **A**, **B** and **C** also experience small changes up to about 150^{th} MD time step. Then, **A**, **B** and **C** increase up to about 10.1 Å. After that, they remain unchanged through the simulation. These changes in angle and length are proof that phase transformation is realized.

The B1 phase of CaS under increased pressure transformed into B2 phase at 170 GPa and we comprehensively analyzed all simulation steps

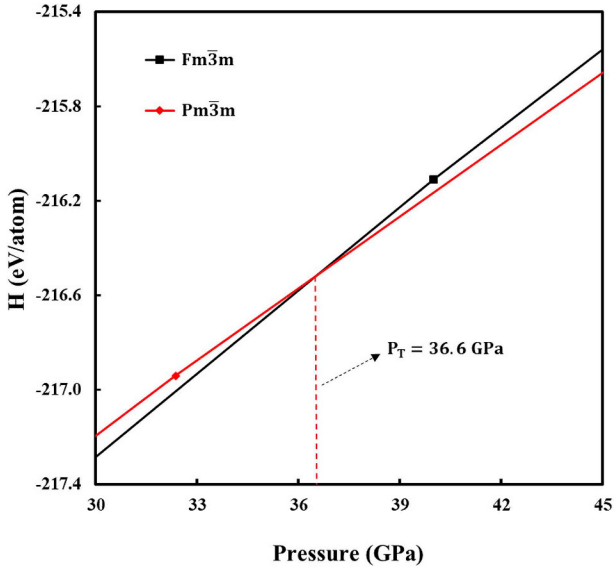

Fig. 4. Enthalpy graph for the stable structural phases of CaS as the function of the pressure.

Table 1
Theoretical (T = 0 K) lattice parameters of CaS for NaCl structure (space group, SG: Fm$\bar{3}$m) and high-pressure phase: CsCl structure (SG: Pm$\bar{3}$m) at the corresponding pressure P_T. *a*, *b*, and *c* are the lattice parameters, B_0 the bulk modulus and B_0 the first derivative of the bulk modulus.

Phases	P_T (GPa)	*a* (Å)	*b* (Å)	*c* (Å)	B_0 (GPa)	B_0'	References
Fm$\bar{3}$m	0	5.7386	5.7386	5.7386	74.08	4.56	This study
		5.4279	5.4279	5.4279	63.80	3.90	[21]
		5.7170	5.7170	5.7170	57.42	3.80	[22]
		5.6890	5.6890	5.6890	64.00	4.20	[23]
		5.6850	5.6850	5.6850	64.85	4.24	[24]
		5.6600	5.6600	5.6600	70.00	4.07	[25]
		5.7200	5.7200	5.7200	56.60	4.12	[26]
Pm$\bar{3}$m	36.60	3.4680	3.4680	3.4680	71.93	4.58	This study
	49.80	3.3234	3.3234	3.3234	66.40	3.90	[21]
	37.22	3.4940	3.4940	3.4940	60.67	3.50	[22]
		3.5190	3.5190	3.5190	77.83	4.23	[24]
	36.85	3.4400	3.4400	3.4400	65.00	4.03	[25]
	36.80	3.4900	3.4900	3.4900	64.50	4.20	[26]

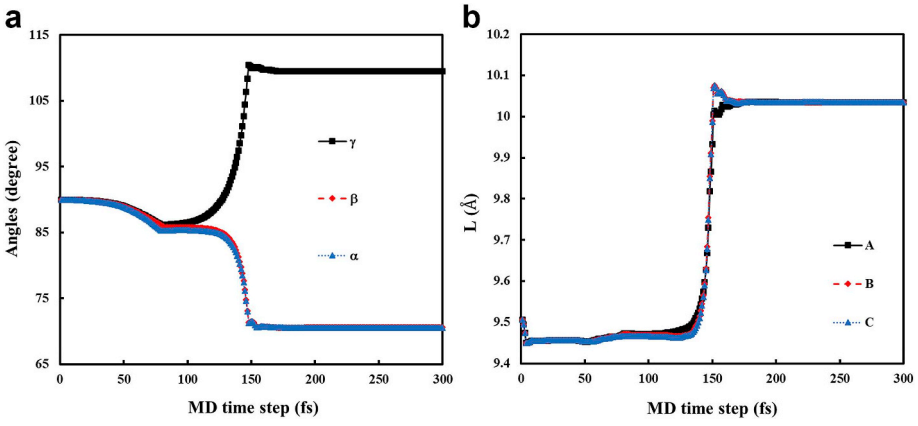

Fig. 5. Lattice vector lengths (a) and the variation of the angles (b) between these vectors of CaS at 170 GPa.

to see if there was any intermediate state during this transform. As a result of analysis that we have done, an intermediate state with the symmetry of R$\bar{3}$m was observed in the 114th simulation step for the resulting B2 structure of CaS. The evolution of the B2 phase is depicted in Fig. 6 and a crystallography table for all calculated structures of CaS is given in Table 2.

The electronic properties such as band structure and density of states (DOS) of CaS calculated for the B1 and B2 structures is shown in

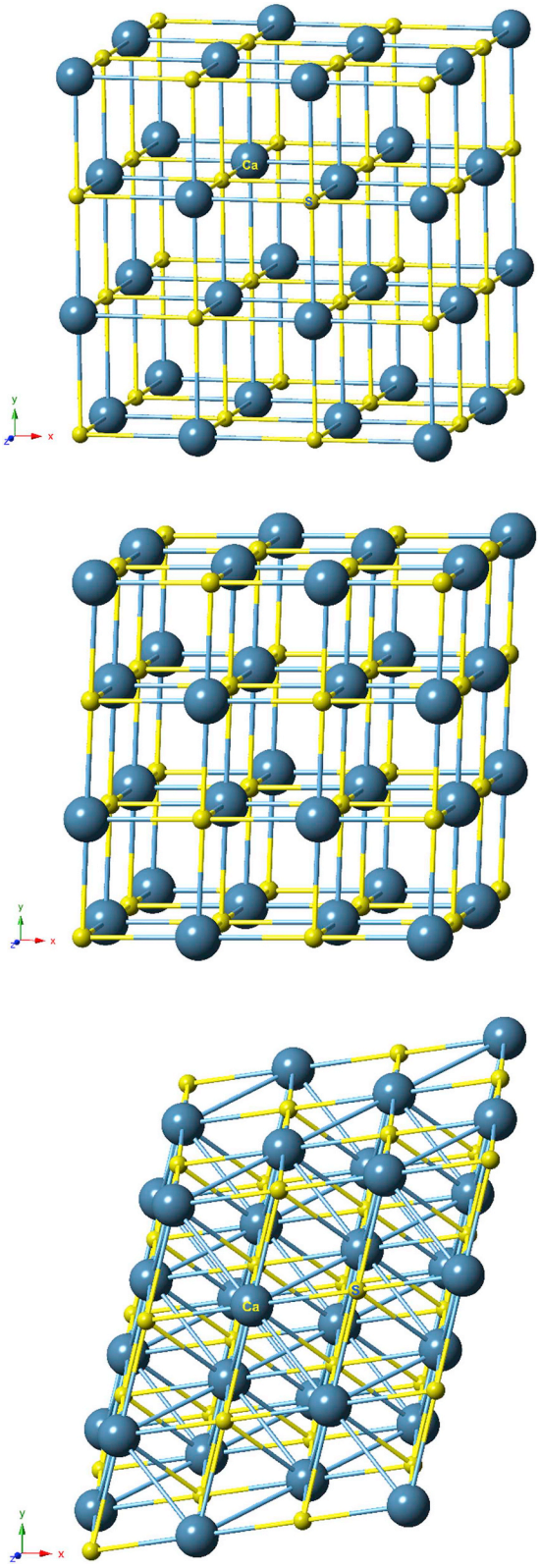

Fig. 6. Formation of CsCl (B2) structure at 170 GPa.

Figs. 7–8 and 9-10, respectively along high symmetry directions and illustrated at the level of Fermi energy as a function of the energy. The Fermi energy level is set to 0 eV. The symmetry points are chosen as W– L– Γ– X– W– K and X– M– R– Γ– R for the B1 and B2 phases, respectively. According to Figs. 7 and 8, B1 and B2 phases of CaS need to be categorized as a typical semiconductor, which exhibit a direct band gap with an energy of 3.77 eV at the Γ-point and 2.09 eV at the R-point of the Brillouin zone, respectively.

Table 2
The calculated space group, lattice parameter, angle, volume and Wyckoff positions values for obtained structures of CaS.

Structures	Space Groups	$a = b = c$ (Å)	$\alpha = \beta = \gamma$	V (Å^3)	Wyckoff Positions
Zinc-blende	F$\bar{4}$3m(No:216)	6.5093	90°	275.81	Ca: 4a 0, 0, 0 S: 4c $\frac{1}{4}, \frac{1}{4}, \frac{1}{4}$
Cubic NaCl (B1)	Fm$\bar{3}$m (No:225)	5.7386	90°	188.98	Ca: 4a 0, 0, 0 S: 4b $\frac{1}{2}, \frac{1}{2}, \frac{1}{2}$
Rhombohedral	R$\bar{3}$m (No:166)	3.9170	62.1807°	60.10	Ca: 1a 0, 0, 0 S: 1b $\frac{1}{2}, \frac{1}{2}, \frac{1}{2}$
Cubic CsCl (B2)	Pm$\bar{3}$m (No:221)	3.4680	90°	41.71	Ca: 1a 0, 0, 0 S: 1b $\frac{1}{2}, \frac{1}{2}, \frac{1}{2}$

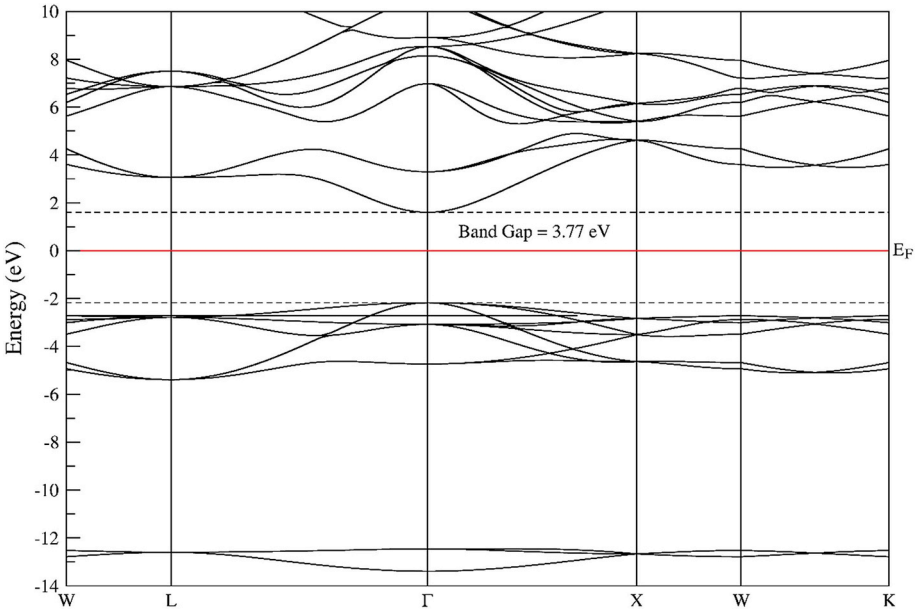

Fig. 7. Band structure for NaCl (B1) structure.

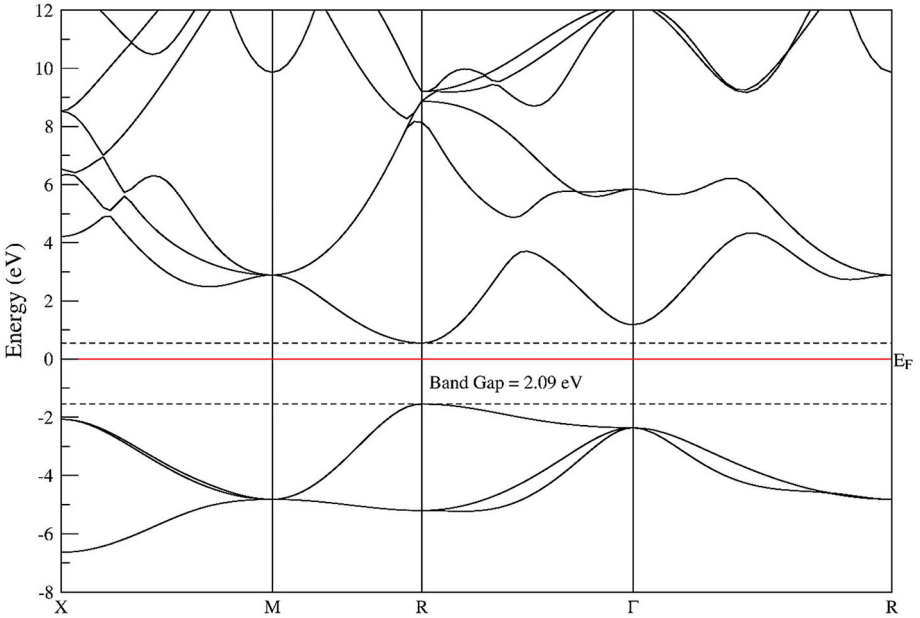

Fig. 8. Band structure for CsCl (B2) structure.

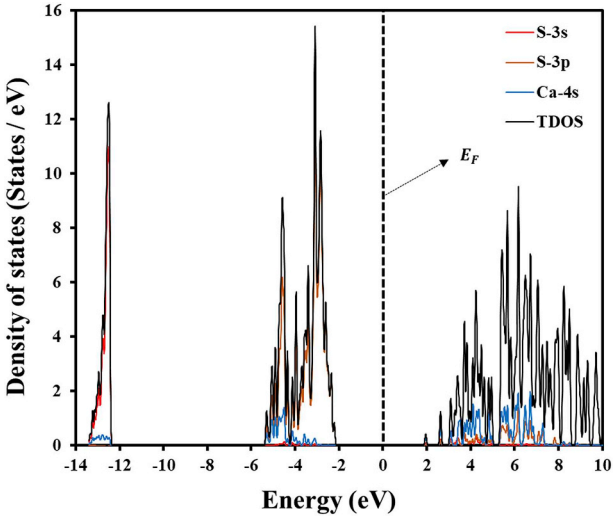

Fig. 9. Density of states in NaCl (B1) structure.

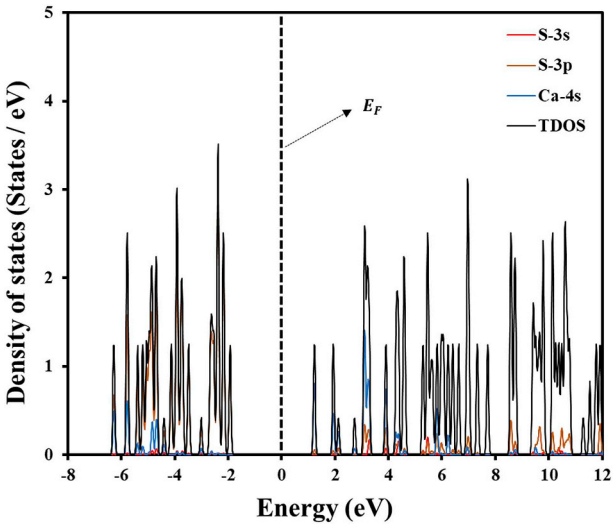

Fig. 10. Density of states in CsCl (B2) structure.

Figs. 9 and 10 show the calculated total and partial DOS of the cubic B1 and B2 phases and are plots of the symmetric bands from −14 eV up to 10 eV for B1 phase and from −8 eV up to 12 eV for B2 phase. As shown in Figs. 9 and 10, the largest contribution came from same states for both B1 and B2 structures (from S-3p states below the Fermi energy level and from Ca-4s above the Fermi energy level).

4. Conclusions

Ab initio calculations using Siesta pocket programme under pressure was applied to study the structural stabilities, phase transitions and electronic properties such as band structure and density of states of the phases of CaS. The transition pressure value was estimated from enthalpy calculations and the effect of hydrostatic pressure on thermodynamics quantities were also studied. Our calculations predict that phase transition from B1 type to B2 type was obtained at 36.6 GPa. The transition pressure, equilibrium lattice constants, bulk modulus and first derivative of bulk modulus values are in good agreement with other theoretical and experimental studies. In addition, an intermediate state was estimated for B2 type structure of CaS for first time.

References

[1] S. Asano, N. Yamashita, Y. Nakao, Phys. Status Solidi 89 (1978) 663–673.
[2] V.S. Stepanyuk, A. Szasz, O.V. Farberovich, A.A. Grigorenko, A.V. Kozlov, V.V. Mikhailin, Phys. Status Solidi 155 (1989) 215–220.
[3] G. Sharma, P. Chawla, S.P. Lochab, N. Singh, Bull. Mater. Sci. 34 (2011) 673–676.
[4] R. Rao, J. Mater. Sci. 21 (1986) 3357–3386.
[5] J. Versluys, D. Poelman, D. Wauters, R.L.V. Meirhaeghe, J. Phys. Condens. Matter 13 (2001) 5709.
[6] S. Hakamata, M. Ehara, H. Kominami, Y. Nakanishi, Y. Hatanaka, Appl. Surf. Sci. 244 (2005) 469–472.
[7] E. Barrett, G.R. Fern, B. Ray, R. Withnall, J. Silver, J. Optic. A 7 (2005) S265.
[8] H. Luo, R.G. Greene, K.G. Handehari, T. Li, A.L. Ruoff, Phys. Rev. B50 (1994) 16232.
[9] N. Troullier, J.L. Martins, Phys. Rev. B 43 (1991) 1993–2006.
[10] P. Ordejon, E. Artacho, J.M. Soler, Phys. Rev. B 53 (R10) (1996) 441–444.
[11] J.P. Perdew, K. Burke, M. Ernzerhof, Phys. Rev. Lett. 77 (1996) 3865–3868.
[12] H.J. Monkhorst, J.D. Pack, Phys. Rev. B 13 (1976) 5188–5192.
[13] R. Hundt, J.C. Schön, A. Hannemann, M.J. Jansen, Appl. Crystallogr. 32 (1999) 413–416.
[14] A. Hannemann, R. Hundt, J.C. Schön, M.J. Jansen, Appl. Crystallogr. 31 (1998) 922–928.
[15] C. Kurkcu, S. Al, Z. Merdan, C. Yamcicier, H. Ozturk, Chin. J. Phys. 56–3 (2018) 783–792.
[16] C. Yamcicier, Z. Merdan, C. Kurkcu, Can. J. Phys. 96 (2) (2018) 216–224.
[17] M. Canpolat, C. Kürkçü, Ç. Yamçıçıer, Z. Merdan, Solid State Commun. 288 (2019) 33–37.
[18] C. Kürkçü, Z. Merdan, Ç. Yamçıçıer, Mater. Res. Express 5 (12) (2018) 125903.
[19] F. Birch, Phys. Rev. 71 (1947) 809–824.
[20] F.D. Murnaghan, Proc. Natl. Acad. Sci. U.S.A. 30 (1944) 244–247.
[21] P.E. Van Camp, V.E. Van Doren, J.L. Martins, Phys. Status Solidi 190 (1995) 193–197.
[22] Z. Charifi, H. Baaziz, F. El Haj Hassan, N. Bouarissa, J. Phys. Condens. Matter 17 (2005) 4083–4092.
[23] P. Cortonay, P. Masri, J. Phys. Condens. Matter 10 (1998) 8947–8955.
[24] H. Khachai, R. Khenatab, A. Haddoua, A. Bouhemadouc, A. Boukortta, B. Soudinia, F. Boukabrined, H. Abida, Phys. Proc. 2 (2009) 921–925.
[25] P. Rodríguez-Hernández, S. Radescu, A. Muñoz, Int. J. High Pressure Res. 22 (2) (2002) 459–463.
[26] A. Shaukat, Y. Saeed, N. Ikram, H. Akbarzadeh, Eur. Phys. J. B 62 (2008) 439–446.